Shielded drive coil & filter stage design for a rabbit sized FFL scanner

G. Bringout, **J. Stelzner**, K. Gräfe and T. M. Buzug

Institut für Medizintechnik, Universität zu Lübeck

Introduction – Coil optimisation

Methods to evaluate the eddy current amplitude induced in a shield are presented. This is used to asses the effect of those currents on the efficiency of coils in an MPI scanner. The example of a shielded drive coil is introduced and a finite element method and a boundary element method are used to evaluate the loss of efficiency of the coil when operated with AC signals.

FEM is used to validate the results of the BEM simulation.

This is done to achieve two goals. First, the reduction of the simulation cost and error, as BEM deals better with integrated quantities as the stored energy in comparison to FEM. Second, the induced current into the shield will be available for further optimization with the BEM formulation

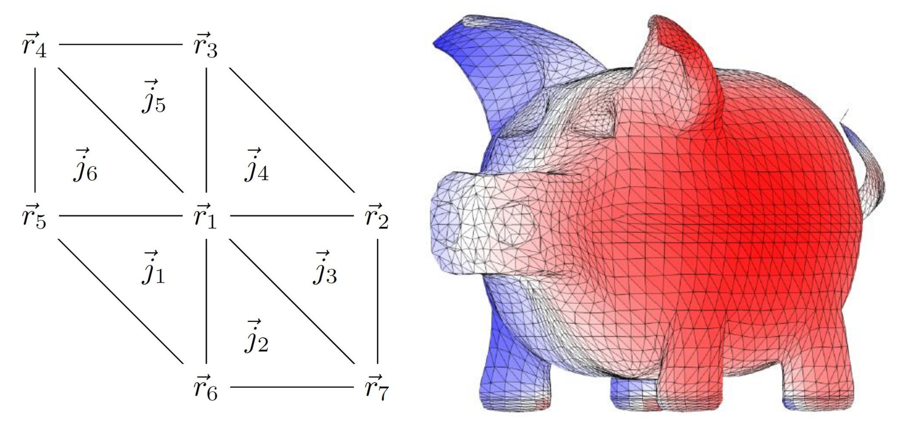

Fig. 1 left: A basic annotated mesh element. A arbitrary surface meshed with triangular elements

To accurately calculate the conductor path on the surface, $\vec{j}$ should be expressed in terms of a stream function ψ [1, 2]. It follows that

$$\vec{j}(\vec{r}) = \mathrm{curl}(\vec{\psi}(\vec{r})\vec{n}(\vec{r})),$$

with $\vec{n}(\vec{r})$ being the normal of the surface *S* at position $\vec{r}$.
Considering *N* nodes with coordinates $\vec{r}_n;\ n = 1, \ldots, N$ on *S*, the function $\hat{\psi}_n$ at node n is defined as

$$\hat{\psi}_n(\vec{r}_j) = \begin{cases} 1 \ if \ j = n, \\ 0 \ if \ j \neq n, \end{cases} \qquad j, n = 1, \ldots, N$$

and $\hat{\psi}_n$ decreases linearly on the edges connected to the node n. The vector $\vec{s} = [s_1 s_2 \ldots s_N]^\intercal$ is called the stream function vector.
The surface current density on the triangle k connected to the nodes $(\vec{r_1}, \vec{r_2}, \vec{r_3})$ with the basis $(\overrightarrow{\psi_1}, \overrightarrow{\psi_2}, \overrightarrow{\psi_3})$ is given by

$$\overrightarrow{j_k} = \frac{s_1\hat{\psi}_1(\vec{r_3} - \vec{r_2}) + s_2\hat{\psi}_2(\vec{r_1} - \vec{r_3}) + s_3\hat{\psi}_3(\vec{r_2} - \vec{r_1})}{\|(\vec{r_2} - \vec{r_1}) \times (\vec{r_3} - \vec{r_1})\|}$$

The surface current density can thus be expressed by

$$\vec{j}(\vec{r}) = \sum_{k=1}^{K} \overrightarrow{j_k}$$

which allows the reformulation of the objective and constraint functions as matrices in the set of basis functions on a mesh.

$$\vec{J} = \vec{j}_1 + \vec{j}_2 + \vec{j}_3 + \vec{j}_4 + \vec{j}_5 + \vec{j}_6.$$

$$\begin{aligned}\vec{J} = &\frac{s_1\widehat{\psi}_1(\vec{r}_3 - \vec{r}_2)}{A_1} + \frac{s_2\widehat{\psi}_2(\vec{r}_1 - \vec{r}_3)}{A_1} + \frac{s_3\widehat{\psi}_3(\vec{r}_2 - \vec{r}_1)}{A_1} + \\ &\frac{s_1\widehat{\psi}_1(\vec{r}_4 - \vec{r}_3)}{A_2} + \frac{s_3\widehat{\psi}_3(\vec{r}_1 - \vec{r}_4)}{A_2} + \frac{s_4\widehat{\psi}_4(\vec{r}_3 - \vec{r}_1)}{A_2} + \\ &\frac{s_1\widehat{\psi}_1(\vec{r}_5 - \vec{r}_4)}{A_3} + \frac{s_4\widehat{\psi}_4(\vec{r}_1 - \vec{r}_5)}{A_3} + \frac{s_5\widehat{\psi}_5(\vec{r}_4 - \vec{r}_1)}{A_3} + \\ &\frac{s_1\widehat{\psi}_1(\vec{r}_6 - \vec{r}_5)}{A_4} + \frac{s_5\widehat{\psi}_5(\vec{r}_1 - \vec{r}_6)}{A_4} + \frac{s_6\widehat{\psi}_6(\vec{r}_5 - \vec{r}_1)}{A_4} + \\ &\frac{s_1\widehat{\psi}_1(\vec{r}_7 - \vec{r}_6)}{A_5} + \frac{s_6\widehat{\psi}_6(\vec{r}_1 - \vec{r}_7)}{A_5} + \frac{s_7\widehat{\psi}_7(\vec{r}_6 - \vec{r}_1)}{A_5} + \\ &\frac{s_1\widehat{\psi}_1(\vec{r}_2 - \vec{r}_7)}{A_6} + \frac{s_7\widehat{\psi}_7(\vec{r}_1 - \vec{r}_2)}{A_6} + \frac{s_2\widehat{\psi}_2(\vec{r}_7 - \vec{r}_1)}{A_6}.\end{aligned}$$

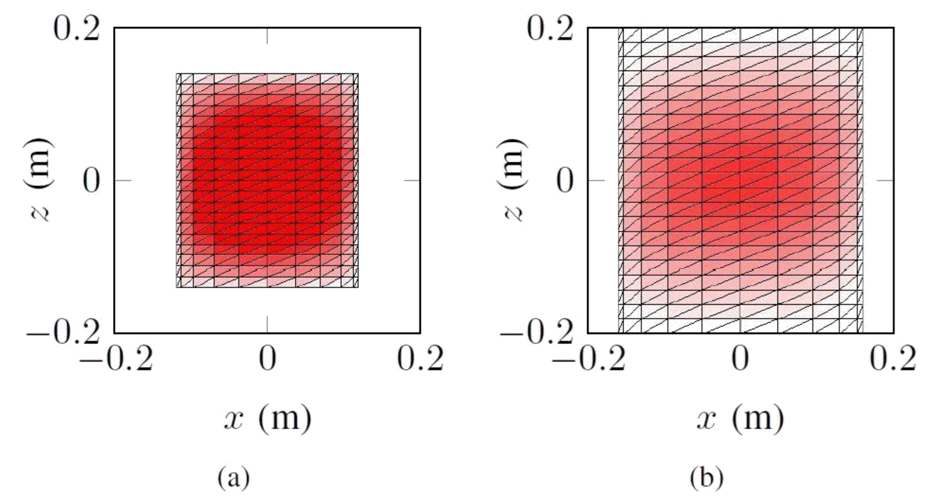

Fig 2. Top views of the stream function amplitude on the meshed surfaces for the coil (a) and for the shield (b). The grey values show the stream function amplitude on the same scale.

Eddy-current estimation & comparison

The vector $\vec{s} = [s_1 s_2 \ldots s_N]^\intercal$ can also be partitioned to reflect the separation of the meshes as

$$\vec{s} = \begin{bmatrix} \vec{s}_s \\ \vec{s}_i \end{bmatrix}.$$

The mutual inductance matrix $\mathbf{M}$ and resistance matrix $\mathbf{R}$ associated to the meshes can also be partitioned as

$$\mathbf{M} = \begin{bmatrix} \mathbf{M}_s & \mathbf{M}_{si} \\ \mathbf{M}_{is} & \mathbf{M}_i \end{bmatrix} \text{ and } \mathbf{R} = \begin{bmatrix} \mathbf{R}_s & 0 \\ 0 & \boldsymbol{R}_i \end{bmatrix}.$$

Here, $\mathbf{M}_s$ and $\mathbf{R}_s$ are the mutual inductance and resistance, respectively, associated to the surface S_s. $\mathbf{M}_i$ and $\boldsymbol{R}_i$ are the ones associated to the surface S_i.$\mathbf{M}_{si}$ is the mutual inductance between the meshes S_s and S_i and $\mathbf{M}_{is} = \mathbf{M}_{si}{}^\intercal$. The matrices $\mathbf{M}_{is}$ and $\mathbf{M}_i$ are symmetric, positive definite and square. Matrix $\boldsymbol{R}_i$ is symmetric, positive semi-definite and square.

To model the time variation of the fields in a representative way for MPI scanners, the example of a drive coil is taken. Those coils are often used with a sinusoidal signal $\vec{s}_s(t) = \vec{s}_s \sin(\omega t)$, with the angular frequency $\omega = 2\pi f$, with f the signal frequency.

The time varying functions $\vec{s}_i(t)$ will then depend on $\vec{s}_s(t)$, $\mathbf{M}_{is}$, $\mathbf{M}_i$ and $\boldsymbol{R}_i$ following the law of conservation of energy as

$$\mathbf{M}_{is}\frac{\mathrm{d}\vec{s}_s}{\mathrm{d}t} + \mathbf{M}_i\frac{\mathrm{d}\vec{s}_i}{\mathrm{d}t} + \boldsymbol{R}_i\vec{s}_i = 0.$$

Solving this allows us to calculate the current density on the shield. For equivalent problem, it took 286 seconds and 160 Mb of memory using this methods and 913 seconds and 12 Gb of memory using COMSOL.

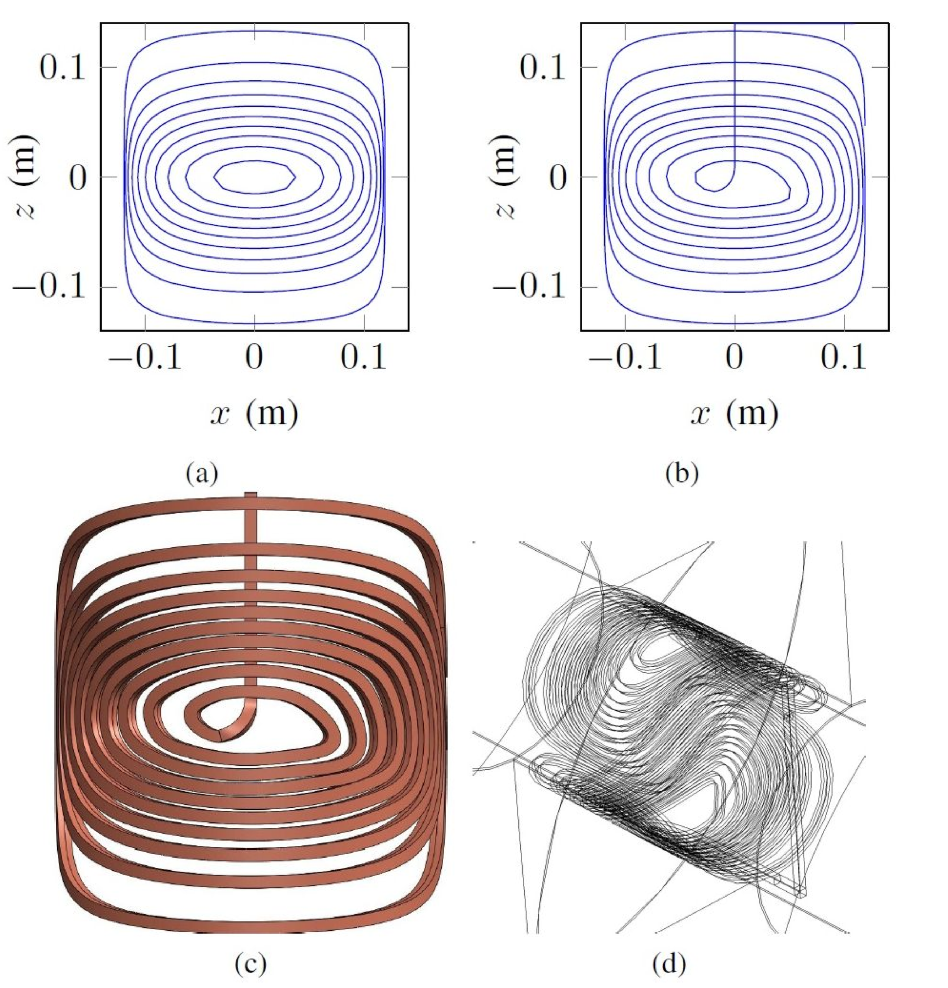

Fig 3. Required data to build the FEM model. (a) The centroids of the ideal current density are calculated. (b) The centroids are connected in order to form a single current path. (c) In a CAD software, the conductor section is swept along the current path. (d) The model is imported into the software and the rest of the geometry is done using the integrated geometry elements.

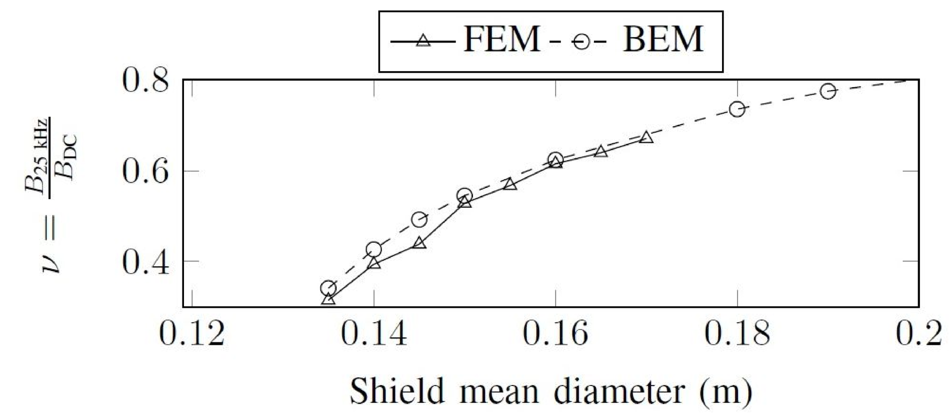

Fig 4. Comparison of the calculation results via FEM and BEM calculations.

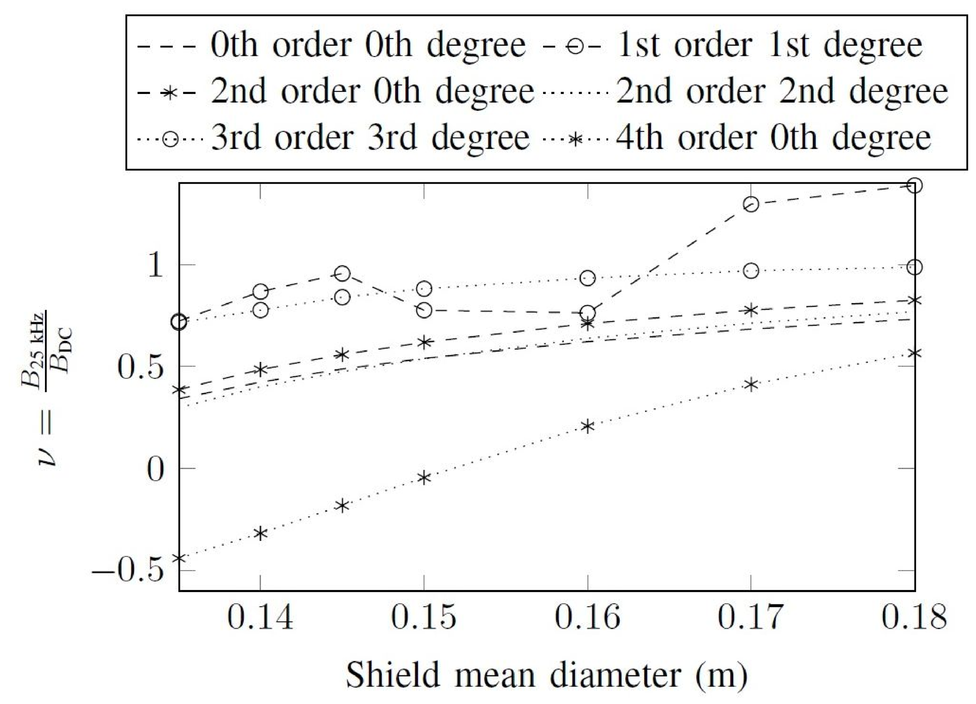

Fig 5. Comparison of the field components having an amplitude higher than 6 uT in BDC. The field topology is slightly changed with change in shield diameter.

Filter coil design

To avoid eddy currents in the surroundings and shielding device, we prefer toroidal coils with nearly no field expansion outside the coil.

In MPI a pure signal of one single frequency is indispensible. To attain such a signal, one needs to attenuate all frequencies outside the desired range, which are generated during the amplification by an electrical filter circuit. The performance of a band pass filter is amongst others affected by the qualify factor of the reactive elements, especially by the serial inductance of the filter coils.

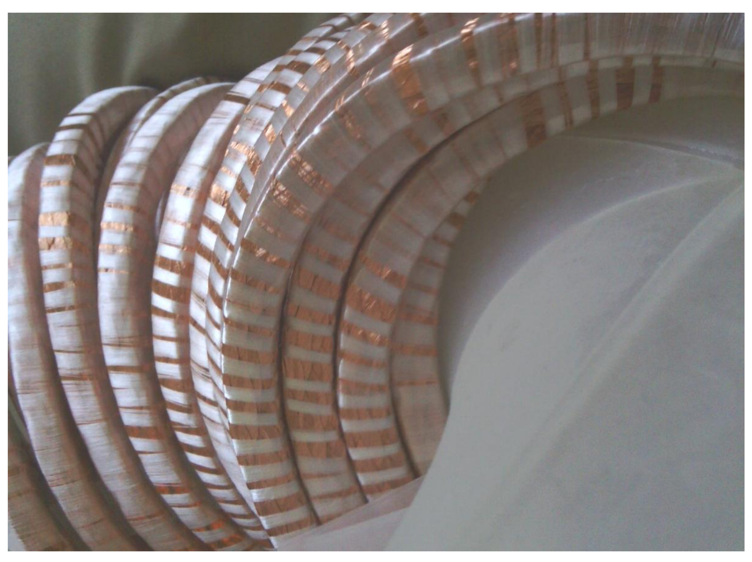

Fig. 6 The winding technique features segments of four Overlapping turns on the inside of the Torus.

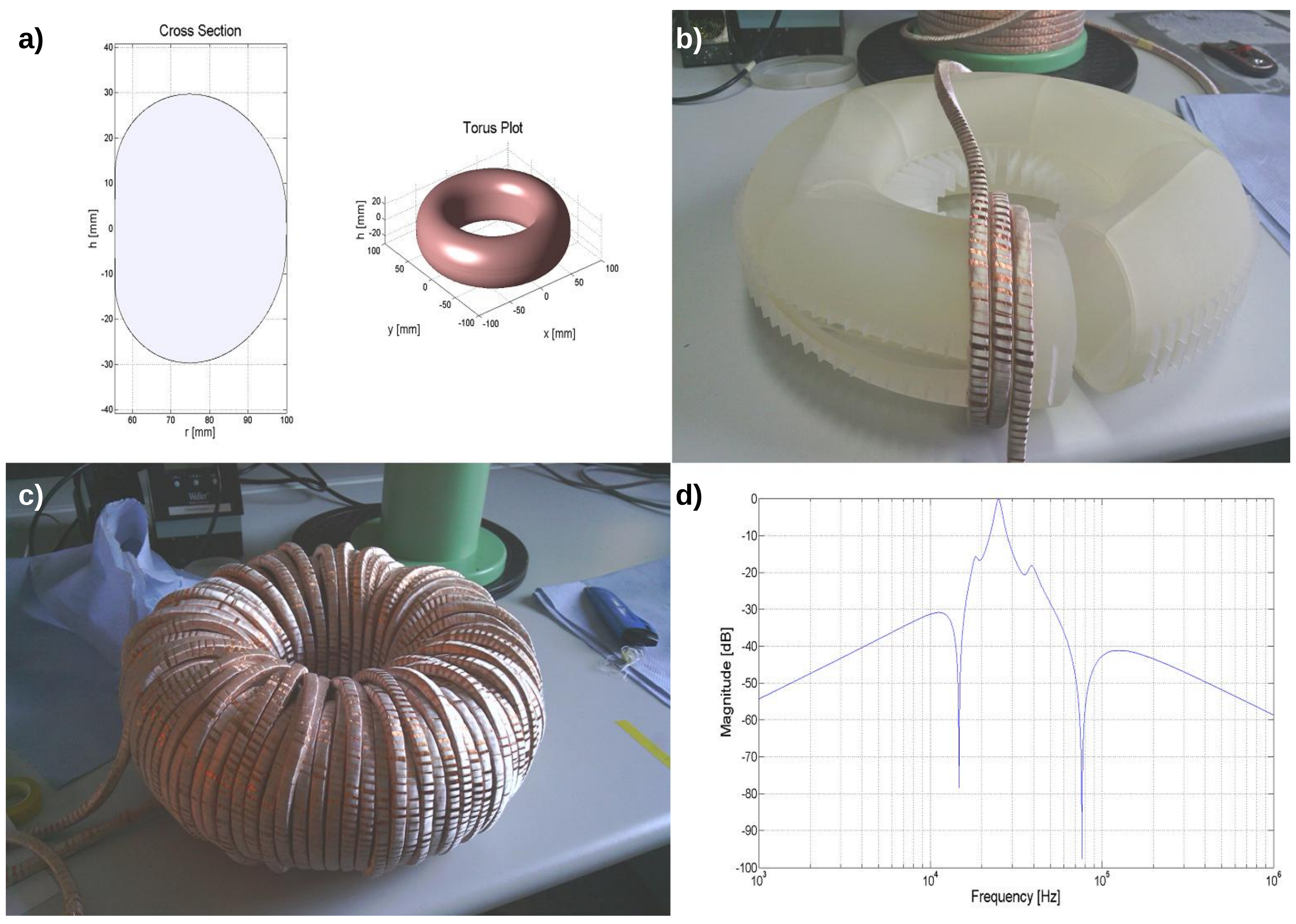

Fig. 7 a) Cross section and 3D Plot of the toroidal shape in MATLAB. b) The unwound Shape was printed by a 3D Printer c) The wound torus with square shaped Litz wire and 104 turns. c) Magnetude against frequency of a calculated filter

The inductance of a toroidal inductor is calculated by [3]

$$L = \frac{\mu_0 N^2}{\pi}\int_{R1}^{R2}\frac{z(r)}{r}dr$$

DC and AC per unit length are described by

$$W_{DC} = \frac{1}{2}\frac{I^2}{\pi a^2 \sigma}$$

$$W_E = k a^4 B_0{}^2 \omega^2 \sigma$$

As the quality factor of an inductor is defined as

$$Q = \frac{2\pi f L}{R_s}$$

the following parameters could be achieved at 25 kHz:

$$L = 164\mu H$$

$$R_s = 47 m\Omega$$

$$Q = 550$$

References
[1] S. Pissanetzky, Minimum energy mri gradient coils of general geometry, *Measurement Science and Technology*, vol. 3, no. 7,1992.
[2] G. N. Peeren, Stream function approach for determining optimal surface currents, Ph.D. dissertation, TU Eindhoven, 2003.
[3] P.N. Murgatroiyd: Some optimum shapes for toroidal incuctors, IEEE Proc., Vol. 129, pp. 168-776, 1982

Acknowledgements
The authors gratefully acknowledge the financial support of the German Federal Ministry of Education and Research (grant numbers 13N11090), the European Union and the State Schleswig-Holstein (grant number 122-10-004).

imt Institut für Medizintechnik
UNIVERSITÄT ZU LÜBECK
INSTITUTE OF MEDICAL ENGINEERING